SAND2018-2673C

DFNE 18–435

DEVELOPMENT AND VALIDATION OF A FRACTURE MODEL FOR THE GRANITE ROCKS AT MIZUNAMI UNDERGROUND RESEARCH LABORATORY, JAPAN

Kalinina, E.A.
Sandia National Laboratories, MS 0779, P.O. Box 5800, Albuquerque, NM 87185, USA
Teklu, H., Wang, Y.
Sandia National Laboratories, MS 0747, P.O. Box 5800, Albuquerque, NM 87185, USA
Ozaki, Y., and Iwatsuki, T.
Japan Atomic Energy Agency, 1-64 Akeyocho, Mizunamishi, Gifu, 509-6132, Japan

ABSTRACT: The Mizunami Underground Research Laboratory is located in Tono area (Central Japan). Its main purpose is providing a scientific basis for the research and development of technologies needed for deep geological disposal of radioactive waste in fractured crystalline rocks. The current work is focused on the experiments in the research tunnel (500 m depth). The collected tunnel and borehole data were shared with the participants of DEvelopment of COupled models and their VALidation against EXperiments (DECOVALEX) project. This study describes how these data were used to (1) develop the fracture model of the granite rocks around the research tunnel and (2) validate the model.

1. INTRODUCTION

The Mizunami Underground Research Laboratory (MIU) is located in Tono area (Central Japan). Its main purpose is providing a scientific basis for the research and development of technologies needed for deep geological disposal of radioactive waste in fractured crystalline rocks. The site hydrology is described in Iwatsuki et al., 2005 and Iwatsuki et al., 2015.

A large amount of fracture data was collected in the Tono area. The fracture data analysis and development of the fracture models at the different scales is an ongoing effort. Bruines et al., 2014 described the development of the discrete fracture network models for 2 scales – local (9km x 9km) and site-scale (2km x 2km). Both models extend from the surface to the depth of 2 km and are based on the data from MIU Project Phase I and II investigations.

The fractured rocks are composed of Toki granite. The upper portion of the Toki granite, known as the Upper Highly Fractured Domain (UHFD), is better characterized. Significantly less data is available for the lower portion, known as Lower Sparsely Fractured Domain (LSFD). Some data for LSFD can be found in JAEA report (Ando et al., 2012) for boreholes DH-2, DH-15 and MIZ-1.

The current work at the MIU is focused on the experiments in the research tunnel (500 m depth). The modeling domain considered in this study is within the LSFD and includes the area surrounding the research tunnel. The model occupies a very small volume of the site-scale model considered in Bruines et al., 2014.

The data used to develop the fracture model are primarily based on the Research tunnel fracture traces and fracture observations in borehole 12MI33. A portion of borehole MIZ-1 is within the modeling domain. The other boreholes are outside the modeling domain. These data were shared with the participants of DEvelopment of COupled models and their VALidation against EXperiments (DECOVALEX) project.

2. APPROACH TO DEVELOPING DISCRETE FRACTURE NETWORK

The discrete fracture network (DFN) model was developed for the area surrounding the MIU Research tunnel at 500 m depth using FRACMAN (Golder Associates, Inc., 2017). This model will be a major tool for simulating hydrogeologic and geochemical conditions in the various experiments being conducted in the Research tunnel. The observed inflow into the tunnel during the excavation was used to validate the model.

The modeling domain is 100x150x100m with the main experimental part of the tunnel, Closure Test Drift (CTD), located approximately in the center. Figure 1 shows the modeling domain, the research tunnel (CTD and Inclined Drift), the horizontal monitoring borehole 12MI33 (with 6 test intervals), and the vertical exploratory borehole MIZ-1 (only 2 test intervals are inside the modeling domain).

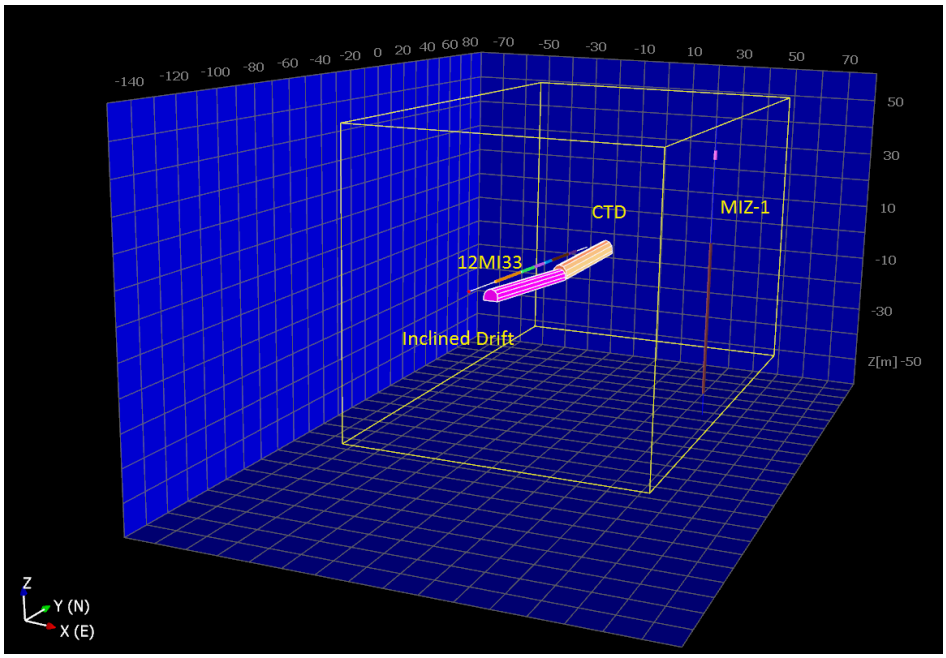

Figure 1. Modeling domain and location of research tunnel and boreholes.

The following data were used in the fracture analysis:

- Fracture traces on the walls of CTD, Inclined Drift, and Access Drift. Note that Access drift fracture data were used in the analysis even though this drift is outside the modeling domain.
- Fractures observed in borehole 12MI33.
- Packer test data in 6 test intervals of 12MI33.

- Measured inflow into the research drift.

Two thousand and twenty three fractures were observed on the wall of the research tunnel. It was assumed that the fractures that did not exhibit any flow discharge are either closed fractures or small fractures not connected to the fracture network. There are 146 fractures (7.2%) with the observed flow discharge. They are characterized in the original data set based on the flow range as "flow" (F) fractures (>1L/min), "drop" (D) fractures (>0.1L/min), and "wet" (W) (<0.1L/min) fractures.

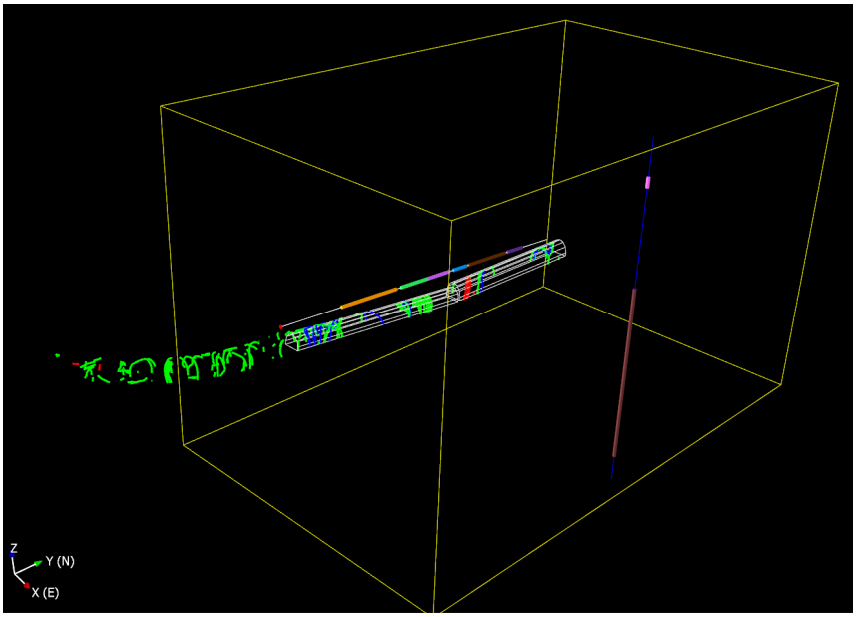

Note: F-fractures are shown in blue, D-fractures are shown in green, and W-fractures are shown in red color.

Figure 2. Traces of the fractures on the Research tunnel walls included in the analysis.

The fracture size was derived from the trace length analysis. It was assumed that the fractures with different flow discharges may have different sizes. Consequently, the analysis was conducted separately for F-, D-, and W- fractures. The trace length distributions of all sets are best described with the lognormal distribution (Table 1). The distributions of W- and D- fractures are very similar and were combined in one. The F- fractures with greater flow rates are also the ones with the larger size.

Table 1. Equivalent fracture radius distribution parameters.

Fracture Set	Distribution Type	Mean Radius (m)	Standard Deviation (m)
D- and W-Fractures	Lognormal	1.42	1.29
F-Fractures	Lognormal	3.88	2.15

The initial evaluation of fracture transmissivity was based on the observed range of flow through the different types of fracture. The analytical solution for the unit inflow (Q) into a circular tunnel with radius r located at depth h (Butscher, 2012) is:

$$Q = \frac{2\pi k(A+H)}{\ln(\frac{h}{r}+\sqrt{\frac{h^2}{r^2}-1}} \quad , \qquad (1)$$

where k is the hydraulic conductivity, H is hydraulic head, and A is defined as:

$$A = h(1-\alpha^2)/(1+\alpha^2) \text{ and } = \frac{1}{r}(h - \sqrt{h^2 - r^2} \qquad (2)$$

The inflow through the fracture (Q_{fr}) with aperture b is:

$$Q_{fr} = Q \cdot b = \frac{2\pi T(A+H)}{\ln(\frac{h}{r}+\sqrt{\frac{h^2}{r^2}-1}} \qquad (3)$$

where $T = k \cdot b$ is fracture transmissivity.

The lower (or upper) fracture transmissivity limit T was calculated from Eq. 3 assuming r= 2.5 m, h=500m, and H=110m. The transmissivity of F- fractures (Q_{fr} > 1.0 L/min) is > $2.6*10^{-8}$ m^2/s, transmissivity of D- fractures (Q_{fr} > 0.1 L/min) is > $2.6*10^{-9}$ m^2/s, and the transmissivity of W- fractures (Q_{fr}< 0.1 L/min) is < $2.6*10^{-9}$ m^2/s. The observed inflows into CTD and Inclined Drift were used to adjust these limits until the good match was obtained (Table 2). The corresponding transmissivity values are: $6.0*10^{-8}$ m^2/s (F-fractures), $6.0*10^{-9}$ m^2/s (D- fractures), and $2.6*10^{-9}$ m^2/s (W- fractures). Assuming water density of 998 kg/m^3 and water viscosity of 0.001 N s/m^2 the fracture permeability values are: $1.5x10^{-10}$ m^2 (F-fractures), $3.2x10^{-11}$ m^2 (D-fractures) and $1.8x10^{-11}$ m^2 (W-fractures).

Table 2. Comparison of measured and calculated inflow into the Research tunnel.

Research Tunnel Segment	Measured Tunnel Inflow (L/min)	Number of Fractures			Calculated Inflow (L/min)			
		F	D	W	F	D	W	Total
CTD	13	4	15	3	9.2	3.45	0.3	12.95
Inclined Drift	43	14	42	N/A	32.2	9.66	0	41.86

The calculated transmissivity (permeability) represents the average values. There is no enough data to develop probability distributions for these parameters. Very few data are available on fracture aperture. This analysis assumed correlations between the lognormally distributed fracture equivalent radius (R) and fracture permeability (k) and aperture (b) in the following form:

$$k = \gamma_1 \cdot R^{\omega} \qquad (4)$$

$$b = \gamma_2 \cdot R \qquad (5)$$

where γ_1, γ_2, and ω are coefficients.

Equation 3 was used to calculate the inflow through each of 146 fractures generated in the Research Tunnel using the lognormal fracture radius distributions (Table 1). The total calculated inflow was compared to the observed inflow. A good match (113 L/ versus 104 L/min) was obtained with the following coefficient values:

- $\gamma_1 = 1.55x10^{-12}$
- $\gamma_2 = 1.16x10^{-5}$

- ω =2.3

The transmissivity estimates were corroborated by comparing the packer test results with the transmissivity of fractures generated in borehole 12MI33. Borehole 12MI33 is a horizontal borehole that is parallel to the Research tunnel (Figure 1). The packer tests were conducted in 6 test intervals. The test intervals also serve as the monitoring points (for observation of temporal variations in pressure and geochemistry in vicinity of the Research tunnel). Two hundred and ninety seven fractures were recorded in the borehole. The fractures were classified as "crack", "hair crack", "discontinuity crack", and "mineral vein". The fractures described as cracks that had recorded aperture values were assumed to be permeable fractures, such as F-, D-, and W-fractures observed in the Research tunnel.

The fractures generated in the borehole are shown in Figure 3 along with the Research tunnel fractures. Figure 3 also shows the transmissivity of the test intervals obtained in the packer tests. The high transmissivity intervals 1, 2' and 6 coincide with the zones in which fractures generated in both, Research tunnel and borehole, are present. Intervals 2 and 3 intersect a few fractures and their transmissivity is lower. Intervals 4 and 5 do not intersect any of generated fractures and their transmissivity is significantly lower. The locations of 17 fractures generated in borehole 12MI33 are consistent with the locations of fractures in the Research tunnel.

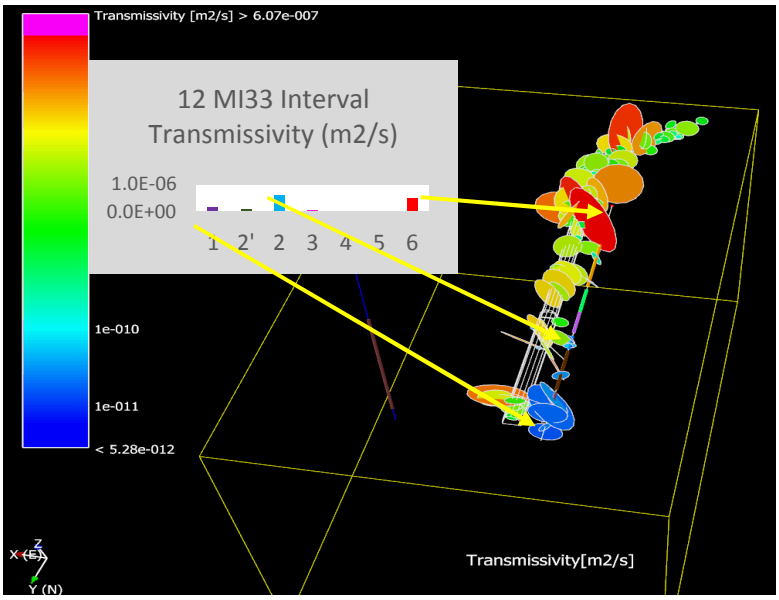

Figure 3. Transmissivity of fractures in the Research tunnel and borehole 12MI33.

The transmissivities of the fractures generated in borehole 12MI33 were compared to the transmissivity of the test intervals from the packer tests in this borehole. The total transmissivity of the fractures generated in the borehole (7.6×10^{-7} m^2/s) is close to the total transmissivity of the test intervals (9.9×10^{-7} m^2/s). Consequently, the fracture properties derived from the Research tunnel fracture trace analysis are consistent with the packer test data in borehole 12MI33.

It can be assumed that the fractures located outside the Research tunnel and borehole 12MI33 have the same parameter distributions as the fractures in the Research tunnel and borehole 12MI33. However, generation of these fractures requires additional parameters, such as the number of fracture sets, orientation distribution of each set, and fracture intensity in each set.

The number of fracture sets and their orientation was obtained from the analysis of the fractures generated from the tunnel traces. Figure 4 shows the fracture set assignment results for the Research tunnel fractures.

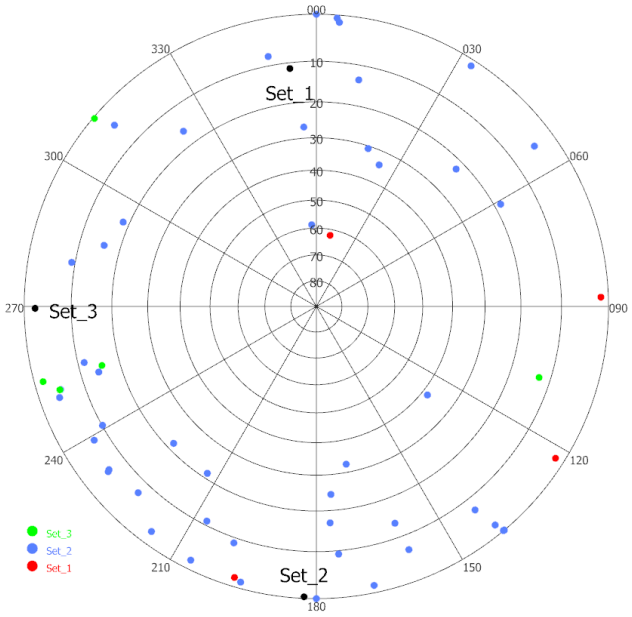

Figure 4. Fracture set assignment results for the Research tunnel fractures.

Three fracture sets were unidentified. The unilateral Fisher's distribution was found to be the best fit for all sets. However, Set 3 in Figure 4 was removed from the analysis. This set contains fractures in the Access Drift. The Access drift is located outside the modeling domain and is affected by the nearby Main Shaft fault.

The properties of the two fractures sets incorporated in the model are provided in Table 3. Note that orientation is given in the local coordinate system. The actual coordinate system was rotated 10.20 clockwise in the x-y plane to align the tunnel with the y axis.

Table 3. Fracture Orientation Distributions.

Fracture Set	Trend (^{0})	Plunge (^{0})	Fisher Dispersion k_f	Volumetric Intensity P_{32} (1/m)
Set 1	208	8	7	0.22
Set 2	303	1.3	3.6	0.086

To evaluate volumetric intensity P_{32} of each fracture set the following approach was used. The stochastic fractures were generated using Fisher distributions (Table 3), fracture radius distributions (Table 1), fracture permeability (Eq. 4), and fracture aperture (Eq. 5). The P_{32} values were iteratively redefined until

the linear intensity (P_{10}) values in two arbitrary placed imaginary horizontal boreholes matched P_{10} of fractures observed in the Research tunnel and borehole 12MI33. The calculated P_{32} values are provided in Table 3.

Figure 5 shows one realization of the DFN generated with the properties defined in Table 3. The DFN also contains fractures generated in the Research tunnel and borehole 12MI33. Figures 6 and 7 show the sampled distribution of fracture permeability and aperture for this realization.

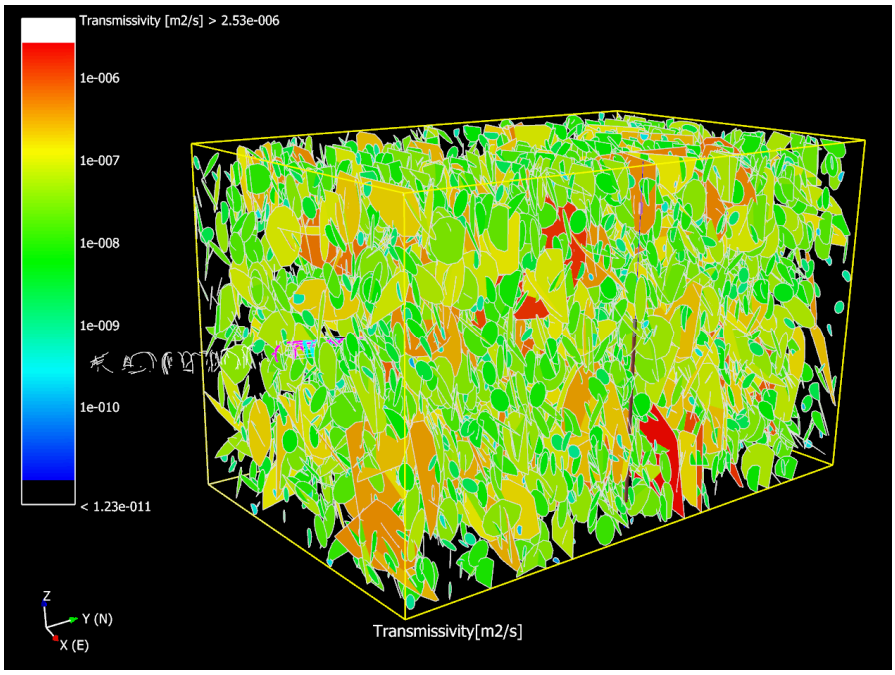

Figure 5. One realization of discrete fracture network.

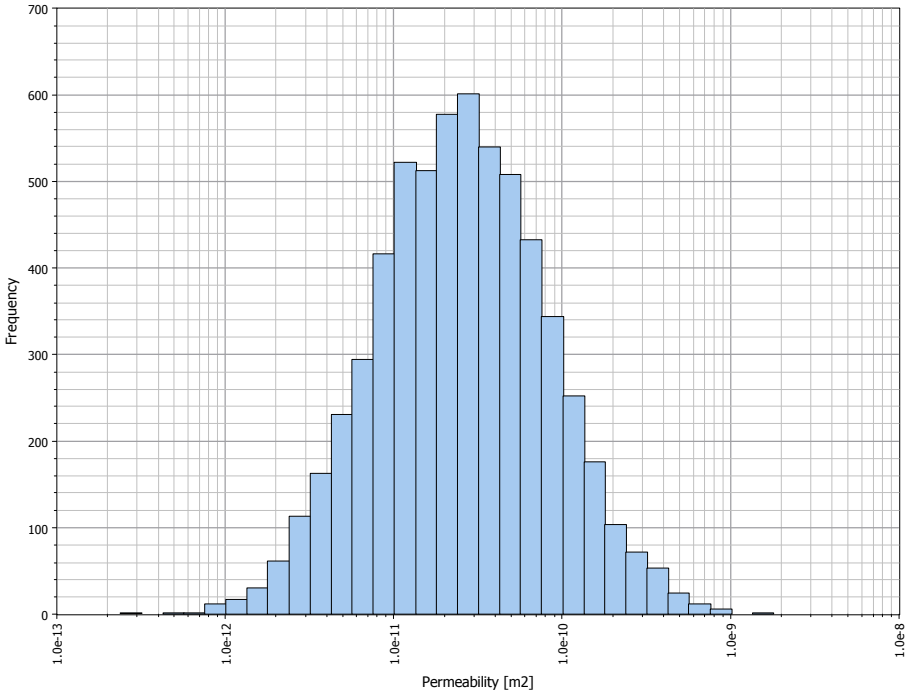

Figure 6. Sampled fracture permeability.

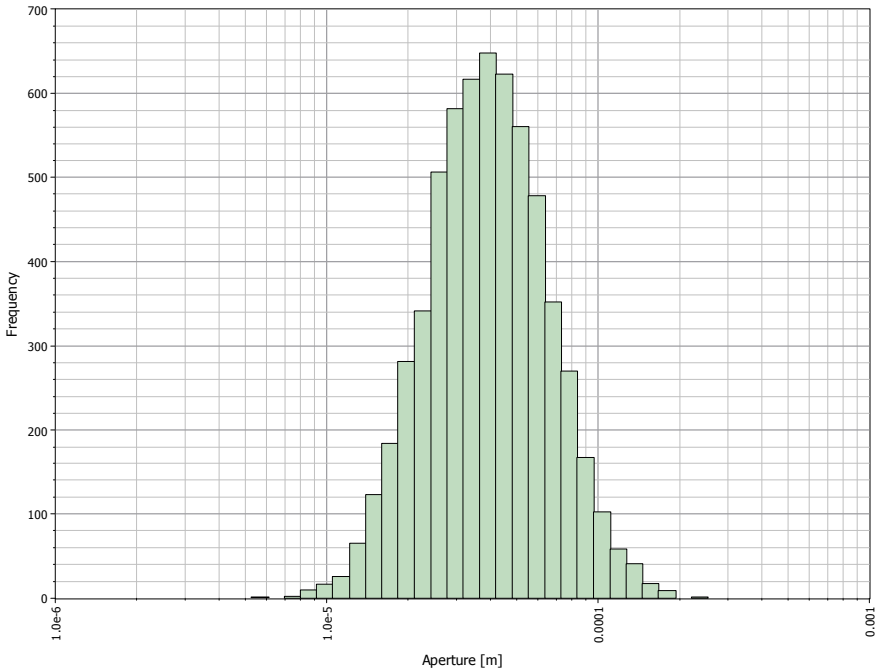

Figure 7. Sampled fracture aperture.

For flow and transport simulations, the DFN was upscaled to an equivalent continuum model with the uniform grid cell size of 1x1x1 m. The effective *x*, *y*, and *z* permeabilities and effective porosity were calculated for each grid cell containing fractures using Oda's method in FRACMAN. The permeability and porosity of the grid cells without fractures were defined in accordance with the matrix permeability and porosity. Figure 8 shows vertical slice of the effective permeability in *z* direction for the DFN realization shown in Figure 5.

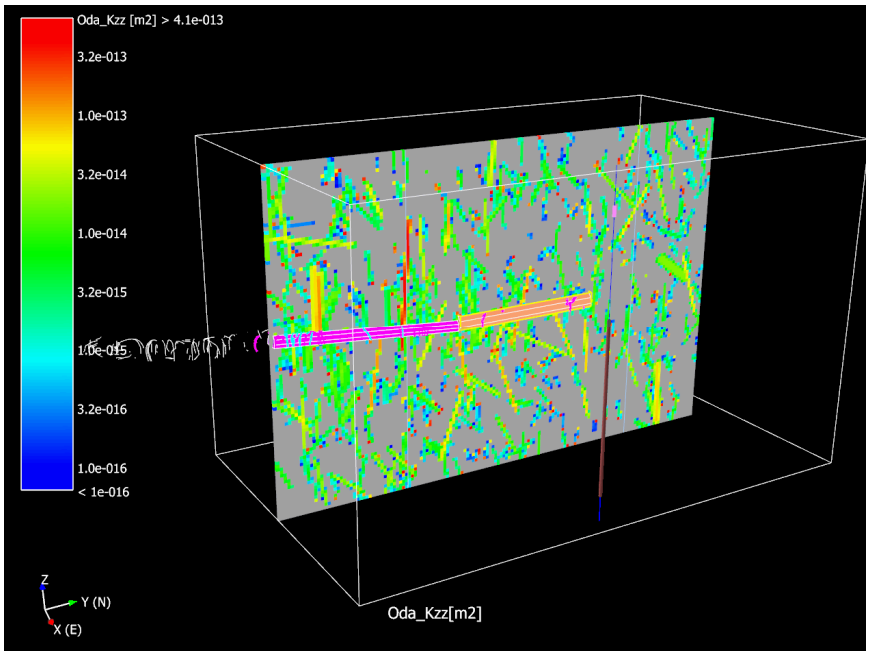

Figure 8. Vertical slice of effective permeability in *z* direction for DFN realization show in Figure 5.

Table 4 summarizes the mean properties of the grid cells in the modeling domain. There is noticeable anisotropy in permeability in *x*. *y*, and *z* directions

Table 4. Effective Continuum Model Mean Grid Cell Properties.

Parameter	Notation	Mean Value
Permeability (m^2)	K_{xx}	3.50E-15
	K_{yy}	1.84E-15
	K_{zz}	4.15E-15
Fracture porosity	€	2.1E-05

3. MODEL VALIDATION

The developed effective continuum model was used to simulate the inflow into the Inclined drift and CTD during the tunnel excavation. The tunnel excavation was modeled by removing material with 1 m increments for a total of 103 m. The flow simulations were conducted with PFLOTRAN (Hammond et al., 2014), an open source, state-of-the-art massively parallel subsurface flow and reactive transport code. The details of flow simulations are presented in a companion paper by Hadgu et al., 2018.

Figure 9 compares the calculated and observed inflows. A very good agreement is obtained with the effective continuum model. Also shown in this figure is the simulation in which a homogeneous model was with permeability of $1x10^{-15}$ m^2 was used. The homogeneous model is not capable of reproducing the observed values as well as the observed trend.

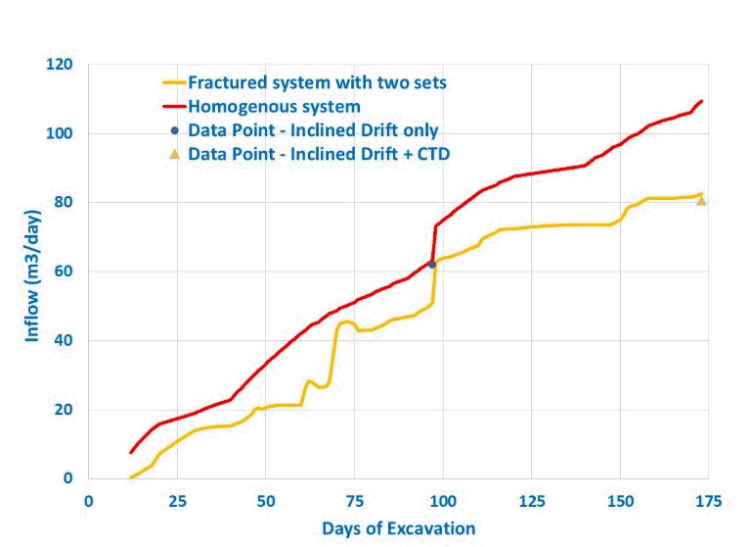

Fig. 9. Predicted and observed inflows into Inclined Drift and CTD.

4. SUMMARY

This analysis demonstrated an approach to developing a small-scale discrete fracture network model around the Research tunnel. The data used included fracture traces mapped on the tunnel walls, fractures observed in borehole 12MI33, packer test results in 6 test intervals of borehole 12MI33, and measured inflow into the different segment of the Research tunnel during the tunnel excavation.

The DFN model includes:

(1) The fractures observed in the Research tunnel and borehole 12MI33. These fractures have deterministic locations and stochastic (radius, permeability, and aperture) properties derived from the fracture analysis.

(2) Stochastic fractures (the location changes with each realization) generated based on the fracture size, orientation, intensity, and properties derived from the fracture analysis.

The DFN model was upscaled to an effective continuum model for flow and transport simulations. The effective continuum model was capable to predict the observed inflows into the tunnel.

5. REFERENCES

1. Ando, K., Tanaka, T., Hashimoto, S., Saegusa, H. and Onoe, H. (2012). Study for establishment of the methodology for hydrogeological modeling using hydraulic discrete fracture networks (study on hydrogeology in crystalline fractured rock), JAEA-Research 2012-022, 2012.

2. Bruines, P., Tanaka, T., Abumi, K., Hashimoto, S., Saegusa, H., Onoe, H., and Ishibashi, M. (2014). Development and Application of the GeoDFN and HydroDFN at the Mizunami Underground Research Laboratory, 8th Asian Rock Mechanics Symposium, October 14-16, 2014, Sapporo, Japan.

3. Butscher, Christoph (2012). Steady-State Groundwater Inflow into a Circular Tunnel, Tunnelling and Underground Space Technology, 32 (2012), pp. 158–167.

4. Golder Associates, Inc. (2017). Interactive Discrete Feature Data Analysis, Geometric Modeling and Exploration Simulation, FracMan Manual, April 6, 2017.

5. Iwatsuki, T.R., R. Furue, H. Mie, S. Ioka, and T. Mizuno. 2005. Hydrochemical baseline condition of groundwater at the Mizunami underground research laboratory (MIU). *J. Applied Geochemistry*. 20(12): 2283–2302.

6. Iwatsuki, T., H. Hagiwara, K. Ohmori, T. Munemoto, and H. Onoe. 2015 Hydrochemical disturbances measured in groundwater during the construction and operation of a large-scale underground facility in deep crystalline rock in Japan. J. *Environmental Earth Sciences*. 74(4): 3041-3057.

7. Hadgu, T, E.A. Kalinina, Y. Wang, Y. Ozaki, and T. Iwatsuki. 2018. Investigations of Fluid Flow in Fractured Crystalline Rocks at the Mizunami Underground Research Laboratory, in Proceedings of the 2nd International Discrete Fracture Network Conference, Seattle, Washington, June 20-22, 2018.

8. Hammond, G.E., P.C., Lichtner, and R.T., Mills. 2014. Evaluating the Performance of Parallel Subsurface Simulators: An Illustrative Example with PFLOTRAN. *J. Water Resources Research*. 50, doi:10.1002/2012WR013483.

ACKNOWLEDGMENT

Sandia National Laboratories is a multi-mission laboratory managed and operated by National Technology and Engineering Solutions of Sandia, LLC., a wholly owned subsidiary of Honeywell International, Inc., for the U.S. Department of Energy's National Nuclear Security Administration under contract DE-NA-0003525. SAND2017- 8240 A.